A LETTERS JOURNAL EXPLORING
THE FRONTIERS OF PHYSICS

OFFPRINT

Wave turbulence observed in an auto-oscillating complex (dusty) plasma

S. ZHDANOV, M. SCHWABE, C. RÄTH, H. M. THOMAS and G. E. MORFILL

Please visit the website
www.epljournal.org

epl

AN INVITATION TO SUBMIT YOUR WORK

www.epljournal.org

The Editorial Board invites you to submit your letters to EPL

EPL is a leading international journal publishing original, innovative Letters in all areas of physics, ranging from condensed matter topics and interdisciplinary research to astrophysics, geophysics, plasma and fusion sciences, including those with application potential.

The high profile of the journal combined with the excellent scientific quality of the articles ensures that EPL is an essential resource for its worldwide audience. EPL offers authors global visibility and a great opportunity to share their work with others across the whole of the physics community.

Run by active scientists, for scientists

EPL is reviewed by scientists for scientists, to serve and support the international scientific community. The Editorial Board is a team of active research scientists with an expert understanding of the needs of both authors and researchers.

epl

A Letters Journal Exploring the Frontiers of Physics

Wave turbulence observed in an auto-oscillating complex (dusty) plasma

S. Zhdanov[1], M. Schwabe[1,2], C. Räth[2], H. M. Thomas[2] and G. E. Morfill[1,3]

[1] *Max Planck Institute for extraterrestrial Physics - PO Box 1312, Giessenbachstr., 85741 Garching, Germany*
[2] *Forschungsgruppe Komplexe Plasmen, Deutsches Zentrum für Luft- und Raumfahrt Oberpfaffenhofen, Germany*
[3] *BMSTU Centre for Plasma Science and Technology - Moscow, Russia*

Abstract – We study a complex plasma under microgravity conditions that is auto-oscillating due to a heartbeat instability and contains quasi-solitary wave ridges —oscillons. We demonstrate that this system can serve as a nearly ideal model system to mimic weak Kolmogorov-Zakharov– type wave turbulence. The slopes of the structure functions agree reasonably well with power laws assuming extended self-similarity. The energy spectrum displays multiple cascades, which we attribute to the influence of friction, the heartbeat instability and a modulational instability.

Introduction. – Complex plasmas consist of micro-meter-sized particles embedded in a low-temperature plasma and are ideal model systems for nanofluids, phase transitions, transport processes, etc. [1]. As an example of complex system dynamics, these solid particles immersed into a weakly ionized plasma are the subject of many detailed studies [1,2]. The microparticles can be visualized individually in real time, thus providing a kinetic level of observations of, for instance, vortices, self-propelling, tunneling and channeling [3–6].

Turbulence in complex plasmas can be triggered by waves or instabilities [7–11]. In contrast to traditional experiments on turbulence (see, *e.g.*, [12–14]), experiments with complex plasmas make the direct imaging of the mutually interacting particles possible. These unique properties allow us to suggest that complex plasmas might also serve well as model systems to link turbulence theory and experiment. To actualize this link in all experimentally necessary details is still challenging in many aspects [15]. It is important to mention that complex plasmas are often dynamically highly dissipative systems. Therefore, one has to think about means to compensate for frictional dissipation. One of the promising examples helping to study *forced turbulence* is to use a marginally unstable system, *e.g.*, a "heartbeat" auto-oscillating complex plasma [16,17]. The heartbeat wave pattern, a succession of contractions and expansions of the particle cloud comprising propagating waves, is closely bound to the

surrounding plasma feeding it [18]. Note that parametrically excited waves are a ubiquitous phenomenon observed in a variety of physical contexts, *e.g.*, for Faraday waves, surface ripples and capillary waves [14,19], and many others.

Specifically, driven turbulence in complex plasmas is of low Reynolds numbers (low-$\mathcal{R}$), which is common in viscoelastic fluids [20]. Complex plasmas are intrinsically non-Newtonian, for instance, they display shear-thinning effects [6,21]. The opportunity to study low-$\mathcal{R}$ turbulence on the "atomistic" level is of great interest in applications as diverse as smart micro-devices, bacterial turbulence, insects flight, large-scale vortex instabilities, etc. [22–25]. Undriven, incompressible Kolmogorov flow in two-dimensional strongly coupled dusty plasmas was recently studied in [11]. Simulations of vortices in complex plasmas to investigate the onset of turbulence and collective effects were performed in [6].

The theory of weak turbulence [26,27] was successfully applied to explain deep-water wave turbulence [27], acoustically induced micro-scale capillary wave turbulence [28], water surface Faraday wave turbulence [19], and in many other numerous applications [15]. The auto-oscillating complex plasma gives one more non-trivial example, as we shall demonstrate in this paper.

Experiment particulars. – We use the experimental data obtained with the PK-3 Plus laboratory operated on
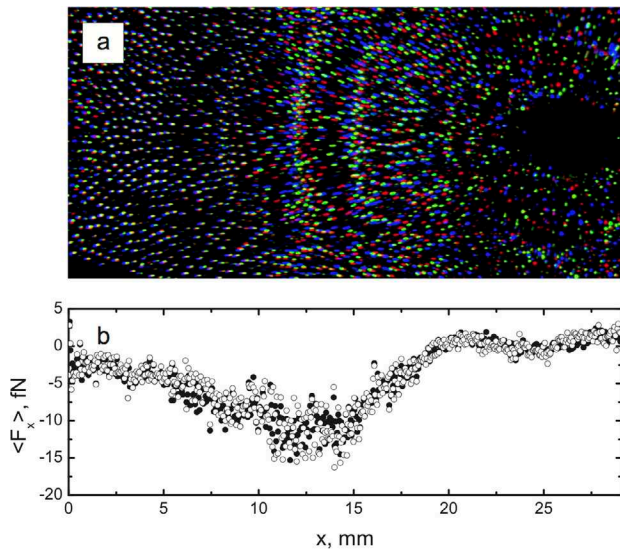
Fig. 1: (Color online) Positions of the particles inside the cloud and the mean force driving oscillations. (a) Imposed three one-period–shifted images taken from three consecutive periods of particle oscillations at the phase of maximal open void (dark region to the right). The field of view is $1.17 \times 2.92\,\mathrm{mm}^2$. The images were RGB-coded to emphasize particle movements. The oscillons are distinctly seen as somewhat denser nearly vertical strips propagating leftwards (at a speed of about 0.4 mm/s [16]). See also the movie `turb.mp4` (1.6 MB). (b) The time (vertical) space averaged horizontal component of the driving force. Bold (open) dots: the forces computed taking into account all particles tracks longer than 5 (10) time steps.

board the International Space Station. Technical details of the setup can be found in [29]. The present experiment was performed in argon at a pressure of 9 Pa [16,17]. The discharge was ignited with a peak-to-peak voltage of 37 V at an applied (rms) power of 0.181 W. Melamine-formaldehyde particles with a diameter of $(9.2 \pm 1\%)\,\mu\mathrm{m}$ and a mass density of $1.51\,\mathrm{g\,cm}^{-3}$ were inserted into the chamber. Their charge was about 9000 electrons/particle. They formed a cloud stretched horizontally with a visibly pulsating elliptically shaped void; see fig. 1(a). The interparticle separation averaged over the entire cloud area was about $230\,\mu\mathrm{m}$. The estimated plasma density and the electron temperature are $n_e \cong 10^8$ cm^{-3}, $T_e \cong 2$–3 eV. Under these conditions, the dust plasma frequency is calculated to be $f_{dust} = 14$–20 Hz, and the dust sound speed $C_{DAW} = 6$–$7\,\mathrm{mm\,s}^{-1}$, which is in a fairly good agreement with measurements [16]. The neutral gas exerted a friction force with a damping rate of about $\gamma_{damp} = 10.7\,\mathrm{s}^{-1}$ [30] on the microparticles. The present discharge regime allows to observe stable long-term oscillations at a fundamental frequency of $f_{HB} = 2.81 \pm 0.03$ Hz, a manifestation of the so-called "heartbeat instability" [29]. In contrast to [16,17], a refined tracking procedure was implemented to improve the tracking accuracy [31].

Force distribution. – The driving force is a necessary element of any self-sustaining oscillatory pattern in
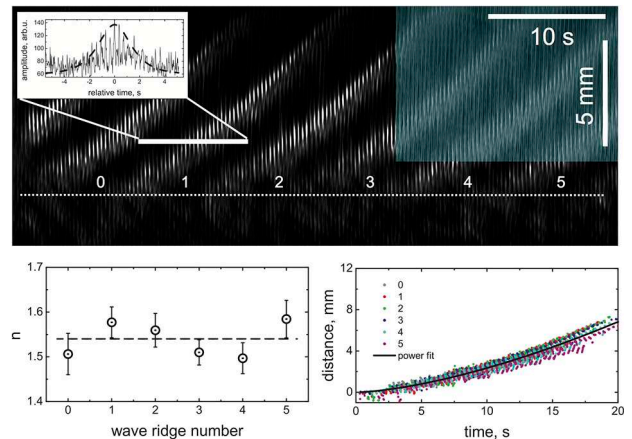

Fig. 2: (Color online) Top panel: time-space plot of the oscillons' wave ridges. The image was preprocessed[1]. To compare, the upper right part is shown as untouched. Compact wave packets (oscillons [16] or quasisolitons [27]) form at the common origin (indicated by the dotted line) and propagate upwards in the figure. Insert: the oscillon wave form corresponds well to that of the soliton solution obtained in [27]. Bottom right panel: tracks of the wave ridges reduced to common origin; the imposed power fit: $x = a(t/\tau)^{\langle n \rangle}$, $a = 6.8$ mm, $\tau = 20$ s, $\langle n \rangle = 1.54$. Bottom left panel: the power-law fitting results of individual wave-ridge tracks (numbered as shown in the top panel), $x \propto t^n$; the dashed line indicates the mean value $\langle n \rangle = 1.54 \pm 0.04$.

dissipative non-linear systems [32,33]. In our case it can be computed by using the relationship $\langle F_x \rangle = M\gamma_{damp}\langle V_x \rangle$, where $M \simeq 0.61$ ng is the particle mass and V_x the horizontal projection of the particle velocity. To lower the noise, the particle tracking data were averaged over about 28 oscillation periods, then binned horizontally (x-direction in fig. 1) and averaged vertically. For the averaging procedure, the data points were selected inside the symmetric (with respect to the void center height) horizontal slice with vertical width of about 11 mm, see fig. 3. The obtained mean-field force distribution is shown in fig. 1(b). To check the tracing quality and the statistical plausibility of the data [34], we compare the results of computations performed using the tracks of the particles traceable for no less than 5 or 10 frames, and observe a fairly good agreement, see fig. 1(b).

The area containing an essentially non-zero mean driving force is designated "dynamical range". We choose it to be located at $2 < x < 20$ mm, see fig. 1(b), rather far away from both the void boundary ($x > 22$ mm) and the cloud edge self-excitations ($x < 0$; not shown in the figure). Inside this range the force distribution is almost triangular in

---

[1]Fit preprocessing procedure: The original time-space plot (see [16,17]) was contrasted and sharpened, smoothed to dissolve "hot" pixels, then truncated and digitalized. The obtained numerical functions $x(t)$ were subjected to the standard two-parametric (A, n) fitting procedure $x - x_k = A(t - t_k)^n$ performed at starting point $x_k = $ const fixed spatially for all wave ridges but periodically distributed over time t_k with a period of 8 s; $t_0 = 0$ for the "0"-wave ridge.

shape. Therefore, it can be well fitted assuming constant slopes (spring constants) of the force distributions leftward or rightward of some "crossroad" point x_c:

$$\partial_x \langle F_x \rangle = \begin{cases} -k_1, & \text{for} \quad x < x_c, \\ k_2, & \text{for} \quad x > x_c, \end{cases} \tag{1}$$

where $k_1 \simeq 690\,\text{eV/cm}^2$, $k_2 \simeq 1300\,\text{eV/cm}^2$, $x_c \simeq 13\,\text{mm}$. Note that the spatial distribution of the driving force resembles well that measured in microgravity conditions for the "trampoline effect" [35]. This analogy allows us to not only reproduce particle migrations in detail but also to explain the origin of the instability by the presence of a little "potential knoll" (on average in time) located in the center of the cloud. The driving force is comparatively small. It is $\langle |F_x| \rangle \simeq 6.5\,\text{fN}$ on average over the dynamical range, that is about 0.11% of the force of gravity, Mg. Still, this kind of "effective gravity", being principally non-zero, enables an energy gain to feed the oscillations.

Oscillons as quasisolitons. – The homogeneity of the observed heartbeat oscillatory field is broken by the spontaneous appearance of higher density stripes —oscillons, which are clearly seen in the center of fig. 1(a)[2]. These pulse-like vertically elongated constrictions are formed repeatedly in the central part of the cloud, then slowly drift outwards. We use a time-space plot to study their kinematics [17,36][3]. The brighter regions of the resulting map correspond to higher particle densities. In our case this dynamical pattern is fine-structured; see fig. 2, top panel. The brighter spikes in the middle (indicating enhanced particle density) are oscillons propagating towards the outer edge of the cloud (that is, upwards in the figure) away from the pulsating void (on bottom). The particles between the spikes where the cloud density is lower are accelerated to supersonic velocities. This indicates a strong local sporadic imbalance between the electric-field force, confining the particles, and the ion drag force, pushing them away from the void [16,17]. Every oscillon is shaped as an "envelope soliton" with the half-width about 1.5–$2\,\text{s}$ (see left inset in fig. 2, top panel) and its lifetime is about $20\,\text{s}$. The spatial full width of the oscillon core is typically about $w_{osc} = 0.6$–$0.7\,\text{mm}$. Short-wavelength wave tails are also clearly seen behind the oscillons in fig. 2. They indicate that oscillons are able to resonantly excite, transport and radiate linear waves, a mechanism that is well known from quasisolitons [27]. As has been predicted in ref. [37], a turbulent process could exist where radiating pulses dominate the spectral flow.

Effective wave dispersion. – The measured oscillon tracks can be used to learn more about the effective dispersion of waves. (As, for instance, carefully observing expanding ripples across water after an object dropped into it can help one to learn about the dispersion of water ripples and gravity waves [38,39].) The tracks of the oscillons are described well by the non-linear power law dependences $x = Ct^n$ (see bottom panels in fig. 2) with $n \simeq 3/2$ and some constant C. Correspondingly, the phase velocity changes along the track as $V_{phase}(k) \equiv \omega(k)/k = \dot{x} \simeq (3/2)\,Ct^{1/2}$. Using Whitham's definition of the group velocity $V_{group}(k) = x/t$ [39] yields $V_{group}(k) \equiv \partial_k \omega(k) \simeq Ct^{1/2}$. Combining both relations leads to $\omega(k)/k \simeq (3/2)\,\partial_k \omega(k)$, and hence

$$\omega(k) \propto k^{2/3}. \tag{2}$$

As a moderate dispersion law between those of deep-water waves ($\omega(k) \propto k^{1/2}$) and capillary waves ($\omega(k) \propto k^{3/2}$), the notable analytically solvable examples [27], this dispersion law is of great interest for further theoretical explorations. In particular, it could help to draw conclusions about wave processes which entail turbulence; see below. Although the non-linearity of the oscillon track might be partly caused by an inhomogeneity of the driving force distribution, the dispersion law above is probably a fairly good approximation. The inhomogeneity effect is likely not crucial: The oscillons are essentially located in a comparatively narrow domain $8.5 < x < 17\,\text{mm}$ where the mean horizontal velocity is almost constant[4], $|\langle v_x \rangle| \simeq 1.4$ mm/s.

Structure functions. – The spatial distribution of the time-averaged longitudinal velocities of the auto-oscillating particles consisting of the regular component and turbulent pulsations is shown in fig. 3, top panel. First of all, it is natural to suggest that the turbulent pulsations originate from the external normally distributed random forces and the mutual interparticle interactions leading to randomization. This unites auto-oscillating complex plasma turbulence with force-curl mediated turbulence simulated in [6]. Thus, it is instructive to check whether the spectra of the experimental pulsations follow similar distributions at an intermediate scale between the cloud half-size (about 20–30 mm) and the interparticle distance (0.2–0.3 mm). A standard way to do this is to compute the velocity structure functions [40],

$$S_p(r) = \langle |u(r) - u(0)|^p \rangle, \tag{3}$$

where u is the longitudinal velocity component at r, p is the order of the structure function. We calculate the structure functions from the horizontal velocity map (shown in the top panel of fig. 3) by calculating the mean

---

[2]It was evidenced in ref. [17] that the heartbeat instability has certain thresholds to be triggered. Close to the thresholds, the particle cloud could be observed oscillating rather weakly.

[3]The time-space plot is constructed as follows: For each recorded image, a slice is cut out that is narrow in vertical (y) direction and comprises the whole horizontal (x) dimension. For each slice and each x position, the pixel brightness is averaged over y. This results in a function of x that shows the brightness distribution for this particular time moment. The time-space plot is obtained by plotting those lines next to each other in a time sequence.

[4]Actually, in view of non-zero drift it would be better to study the relative movements of the wave ridges. Fortunately, as computations show, this method gives results that differ only about 5–6% from $n \simeq 3/2$. Therefore, in what follows we accept $x \propto t^{3/2}$ and consequently $\omega \propto k^{2/3}$.
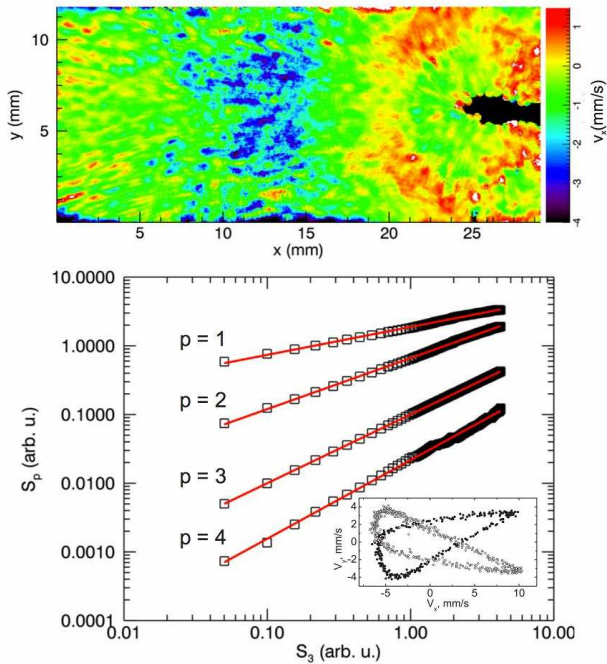
Fig. 4: Velocity fluctuation spectrum (inverse wavelength *vs.* frequency) measured inside the "buffer zone". The $6.4\,\mathrm{mm\,s^{-1}}$-slope dashed line indicates the speed of sound measured in [16]. The resonant amplification of the sound intensity at the frequencies of the heartbeat oscillation harmonics is evident.

Fig. 3: (Color online) Top panel: the time-averaged horizontal velocity map. Bottom panel: (squares) first- ($p = 1$) through fourth- ($p = 4$) order longitudinal velocity structure functions S_p *vs.* S_3, the third-order structure function. The solid lines are the least-square fits with the slopes 0.41 ± 0.01 ($p = 1$), 0.74 ± 0.01 ($p = 2$), and 1.14 ± 0.02 ($p = 4$). For better visibility, the plots were multiplied by the factors 3 ($p = 1$), 0.1 ($p = 3$), and 0.01 ($p = 4$), which does not change their slopes. Inset: phase portraits of two particles located in the buffer zone ($\langle x \rangle = 1.00/1.59\,\mathrm{mm}$, $\langle y \rangle = 0.57/10.4\,\mathrm{mm}$ filled/open dots). Note the intrinsic asymmetry of the dynamical pattern.

velocity differences as a function of horizontal distance only (and tested this method with test images). As observed in simulations [6], the log-log plots of S_p-functions agree reasonably well with power laws assuming the so-called "extended self-similarity" $S_p \propto S_3^{\zeta_p}$ [41]: The slopes of the fits are close to the "classical" Kolmogorov exponents [42] $S_p \propto S_3^{\zeta_p}$, with $\zeta_p = p/3$, though not exactly the same. The fairly good agreement with power laws indicates that this hypothesis works reasonably well. This is actually surprising, because turbulence in an auto-oscillating plasma, like driven turbulence of water Faraday waves [14], is not free, and "*a priori*" the extended self-similarity hypothesis is hardly to be expected to succeed.

The resonant cascade process. – To more closely analyze the structure of turbulence and associated wave processes we study excitations inside the "buffer zone" ($0 < x < 7\,\mathrm{mm}$; see fig. 1), which is relatively tranquil and free of intense non-linear excitations[5]. This enables a closer look at weak fluctuations. The inset in fig. 3

---

[5]The cloud oscillations are influenced by the instability of the entire discharge. It is apparent from observed glow variations which are well correlated with the particle oscillations [17], as well as by the supersonic character of the ion drag force evidenced in [16].
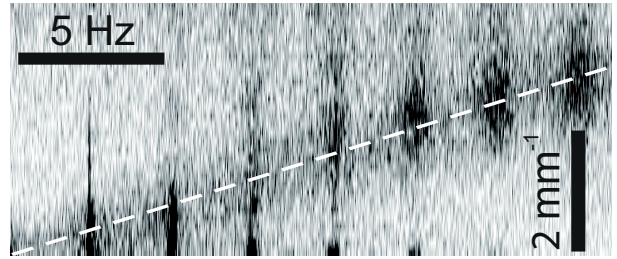
shows the phase portraits of two particles inside the buffer zone. They are oscillating in position, but asymmetrically. Apparently, the buffer zone serves as a transmitter of the wave energy pumped into the system by the auto-oscillating plasma. The parametric process in the energy cascade manifests there by the discrete feature of enhanced harmonics located along the sound branch. Their appearance, hence, indicates a resonant origin of the interactions of sound waves and cloud oscillations. The spectrum shown in fig. 4 resembles spectra of non-linear interactions of longitudinal waves accompanied by wave harmonics generation observed in a two-dimensional plasma crystal [43], and, to some extent, cascade spectra of Langmuir waves detected in ionospheric plasmas heating experiments [44].

Modulational instability. – Even though it can be seen as quite promising, the classical scenario fails to fully describe turbulence in an auto-oscillating complex plasma. Therefore, we shall now consider the influence of the oscillons: They are surprisingly well "channeled", which would lead one to expect that the turbulence might be quasi–two-dimensional to a certain extent. Nevertheless, in our case the oscillons are essentially three-dimensional nearly toroidally symmetric formations, propagating radially inside the cloud; see [16]. Therefore, three-dimensional effects, especially in the short-wavelength domain, are difficult to rule out. The appearance of such "traveling pulses" or quasisolitons is a clear manifestation of the *modulational instability* [27,45], which is ubiquitous in a great number of applications in water waves, plasma waves, optical waves and many others [46]. The oscillons happen to periodically appear, propagate and then fade away in the cloud with a quasi-period of about $8\,\mathrm{s}$. Thus, given $V_{osc} \approx 0.4\,\mathrm{mm/s}$, the distance between the wave ridges is about $l = 3\,\mathrm{mm}$. This gives a time increment of the modulational instability $\gamma_{mi} = C_{DAW}/l \simeq 2\,\mathrm{s^{-1}}$.

Multi-cascade energy spectrum. – An anomalous type of turbulence clearly manifests by the multi-cascade k-spectrum of energy fluctuations. We computed the energy spectrum by using Fourier-transformed mean velocity, namely by associating angle-averaged values of
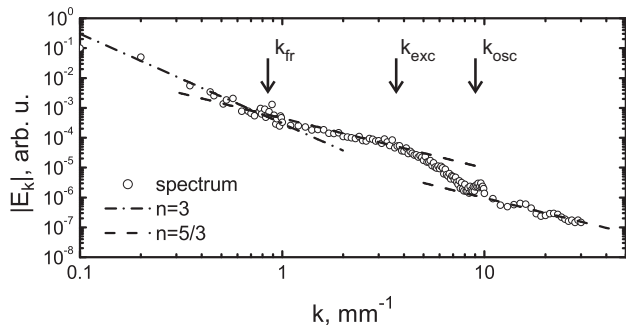
Fig. 5: Fluctuation energy spectrum E_k *vs.* wave number k. The knees on the short-wavelength tail of the spectrum are noticeable. The relevant characteristic wave numbers k_{fr}, k_{exc}, k_{osc} indicated by the arrows are positioned as explained in text. The power-law spectra $\propto k^{-n}$ with $n = 3$ and $n = 5/3$ are shown to guide the eye[6].

$E_k \propto |\mathbf{V_k}|^2$ with every wave vector modulus $k = |\mathbf{k}|$. The log-log plot of the obtained spectrum consists of (practically) constant-slope linked straight lines; see fig. 5. The origin of the knees in the energy spectrum is easy to address. Their position (indicated by arrows in fig. 5) correlates numerically well with the space-scales,

$$k_{fr} = \frac{\gamma_{damp}}{2C_{DAW}} \simeq \frac{2\pi}{L}, \ k_{exc} = \frac{2\pi f_{HB}}{C_{DAW}}, \ k_{osc} = \frac{2\pi}{w_{osc}}. \quad (4)$$

defined by friction, heartbeat excitation and modulational instability[7]. Estimates yield $k_{fr}/k_{exc}/k_{osc} \simeq 0.84/2.7/9.0 \, \mathrm{mm}^{-1}$ for our set of parameters. The slope values are easily recognizable, *e.g.*, the dependence $E_k \propto k^{-5/3}$ is of a "classical" Kolmogorov-type spectrum [42], which is the same in two-dimensional and in three-dimensional turbulence. The crossover for $k < k_{fr}$ to $E_k \propto k^{-3}$ dependence is due to friction [6,40]. The slope change at $k \simeq k_{exc}$ resembles well the double-cascade predicted for forced turbulence in [48]. It is similar to Faraday wave observations [14] where the presence of inverse ($E_k \propto k^{-5/3}$ for $k < k_{exc}$) and direct ($E_k \propto k^{-3}$ for $k > k_{exc}$) energy cascades was identified. The double cascade might also be thought of as appearing due to creation of "coherent condensates" —large-scale accumulation of energy indicating formation of system-sized vortices, zonal flows or similar structures [19,49,50]. In particular, the regular "grid" of oscillon ridges (fig. 2) observed in our case is of the same origin.

Kolmogorov-Zakharov turbulence. – As mentioned above, the oscillons might be thought to be weakly unstable to short-wave perturbations. For instance, in ref. [45] the instability, enhancing short radiating pulses,

has been shown to be crucial for explaining anomalous turbulent behavior. Therefore, it is natural to expect the appearance of the next knee at $k \simeq k_{osc}$ defined by the width of the traveling pulses. Curiously, at $k > k_{osc}$ the slope change resumes the classical $k^{-5/3}$ spectrum. Note an interesting observation. Assuming the short-wavelength fluctuations to be isotropic, and applying an effective dispersion law (2), by using ref. [51] it is straightforward to check that both 3-wave and 4-wave turbulent processes must possess similar spectra. This enables us to come to a rather crucial conclusion: The 3-wave processes are dominant for $k_{fr} < k < k_{exc}$ (in close agreement with expectations [48]), whereas the 4-wave processes dominate the short-wavelength tail of the energy spectrum of weak turbulence at $k > k_{osc}$. The energy is transferred as expected in Kolmogorov-Zakharov turbulence [27].

Summary. – We have explored the low-$\mathcal{R}$ turbulent flow induced by the heartbeat instability in an auto-oscillating complex plasma cloud. The flow reveals a complicated and neatly structured multi-cascade turbulent process. A direct and an inverse energy cascade influenced by friction, modulational and short-wavelength instabilities resulting in a quasi-stationary turbulent state seems to be a promising model able to adequately address all the fine features of the observed particle and energy transport. Our findings certainly indicate a dominant trend $E_k \propto k^{-5/3}$ which, together with an effective wave dispersion $\omega \propto k^{2/3}$ disclosed by propagating oscillons, strictly confirm with "dimensional" arguments proposed in ref. [51] for the Kolmogorov-Zakharov turbulence spectra. These results show that complex plasmas are a promising tool to study turbulence on the level of individual particles. Still many interesting questions remain to be answered, for instance about the onset of turbulence.

$$* * *$$

---

[6]A relatively small range of fluctuation levels (about one order of magnitude in E_k) is not much for a reliable determination of the slope.

[7]Here $L \simeq 7$ cm is the traveling path or, equivalently, the damping length of the waves the oscillon ridges consist of, k_{exc}, "demarcating" the inverse and the direct cascades as evidenced recently in numerical simulations [47], indicates the position of forcing, k_{osc} is defined by the width of the oscillons.

REFERENCES

[1] MORFILL G. E. and IVLEV A. V., *Rev. Mod. Phys.*, **81** (2009) 1353.

[2] SHUKLA P. K. and MAMUN A. A., *Introduction to Dusty Plasma Physics* (Institute of Physics Publishing, Bristol) 2002.

[3] AKDIM M. R. and GOEDHEER W. J., *Phys. Rev. E*, **67** (2003) 056405.

[4] MORFILL G. E., KONOPKA U., KRETSCHMER M., RUBIN-ZUZIC M., THOMAS H. M., ZHDANOV S. K. and TSYTOVICH V., *New J. Phys.*, **8** (2006) 7.

[5] LAUT I., RÄTH C., WÖRNER L., NOSENKO V., ZHDANOV S. K., SCHABLINSKI J., BLOCK D., THOMAS H. M. and MORFILL G. E., *Phys. Rev. E*, **89** (2014) 023104.

[6] SCHWABE M., ZHDANOV S., RÄTH C., GRAVES D. B., THOMAS H. M. and MORFILL G. E., *Phys. Rev. Lett.*, **112** (2014) 115002.

[7] SHUKLA P. K., BHARUTHRAM R. and SCHLICKEISER R., *Phys. Plasmas*, **11** (2004) 1732.

[8] PRAMANIK J., VEERESHA B., PRASAD G. and KAW P., *Phys. Lett. A*, **312** (2003) 84.

[9] PIGAROV A. Y., KRASHENINNIKOV S. I., SOBOLEVA T. K. and ROGNLIEN T. D., *Phys. Plasmas*, **12** (2005) 122508.

[10] TSAI Y.-Y., CHANG M.-C. and LIN I., *Phys. Rev. E*, **86** (2012) 045402.

[11] GUPTA A., GANESH R. and JOY A., *Phys. Plasmas*, **21** (2014) 073707.

[12] ARNÈODO A., BENZI R., BERG J., BIFERALE L., BODENSCHATZ E., BUSSE A., CALZAVARINI E., CASTAING B., CENCINI M., CHEVILLARD L., FISHER R. T., GRAUER R., HOMANN H., LAMB D., LANOTTE A. S., LÉVÈQUE E., LÜTHI B., MANN J., MORDANT N., MÜLLER W.-C., OTT S., OUELLETTE N. T., PINTON J.-F., POPE S. B., ROUX S. G., TOSCHI F., XU H. and YEUNG P. K., *Phys. Rev. Lett.*, **100** (2008) 254504.

[13] MONCHAUX R., *New J. Phys.*, **14** (2012) 095013.

[14] VON KAMEKE A., HUHN F., FERNÁNDEZ-GARCÍA G., MUNUZURI A. P. and PÉREZ-MUNZURI V., *Phys. Rev. Lett.*, **107** (2011) 074502.

[15] SHRIRA V. and NAZARENKO S. (Editors), *Advances in Wave Turbulence*, in *World Scientific Series on Nonlinear Science Series A*, Vol. **83** (World Scientific, Singapore) 2013.

[16] ZHDANOV S. K., SCHWABE M., HEIDEMANN R., SÜTTERLIN R., THOMAS H. M., RUBIN-ZUZIC M., ROTHERMEL H., HAGL T., IVLEV A. V., MORFILL G. E., MOLOTKOV V. I., LIPAEV A. M., PETROV O. F., FORTOV V. E. and REITER T., *New J. Phys.*, **12** (2010) 043006.

[17] HEIDEMANN R., COUËDEL L., ZHDANOV S., SÜTTERLIN K., SCHWABE M., THOMAS H., IVLEV A., HAGL T., MORFILL G., FORTOV V., MOLOTKOV V., PETROV O., LIPAEV A., TOKAREV V., REITER T. and VINOGRADOV P., *Phys. Plasmas*, **18** (2011) 053701.

[18] MIKIKIAN M., COUËDEL L., CAVARROC M., TESSIER Y. and BOUFENDI L., *New J. Phys.*, **9** (2007) 268.

[19] XIA H., FRANCOIS N., PUNZMANN H. and SHATS M., *Nat. Commun.*, **4** (2013) 2013.

[20] GROISMAN A. and STEINBERG V., *Nature*, **405** (2000) 53.

[21] NOSENKO V., IVLEV A. V. and MORFILL G. E., *Phys. Rev. E*, **87** (2013) 043115.

[22] WANG Z. J., *Phys. Rev. Lett.*, **85** (2000) 2216.

[23] CISNEROS L. H., CORTEZ R., DOMBROWSKI C., GOLDSTEIN R. E. and KESSLER J. O., *Exp. Fluids*, **43** (2007) 737.

[24] TIERNO P., GOLESTANIAN R., PAGONABARRAGA I. and SAGUE F., *J. Phys. Chem. B*, **112** (2008) 16525.

[25] TUR A. and YANOVSK V., *Open J. Fluid Dyn.*, **3** (2013) 64.

[26] ZAKHAROV V., L'VOV V. and FALKOVICH G., *Kolmogorov Spectra of Turbulence* (Springer, Berlin) 1992.

[27] ZAKHAROV V., DIAS F. and PUSHKAREV A., *Phys. Rep.*, **398** (2004) 1.

[28] BLAMEY J., YEO L. Y. and FRIEND J. R., *Langmuir*, **29** (2013) 3835.

[29] THOMAS H. M., MORFILL G. E., FORTOV V. E., IVLEV A. V., MOLOTKOV V. I., LIPAEV A. M., HAGL T., ROTHERMEL H., KHRAPAK S. A., SÜTTERLIN R. K., RUBIN-ZUZIC M., PETROV O. F., TOKAREV V. I. and KRIKALEV S. K., *New J. Phys.*, **10** (2008) 033036.

[30] EPSTEIN P., *Phys. Rev.*, **23** (1924) 710.

[31] HEIDEMANN R., ZHDANOV S., SÜTTERLIN K. R., THOMAS H. M. and MORFILL G. E., *EPL*, **96** (2011) 15001.

[32] BONILLA L. L. and GRAHN H. T., *Rep. Prog. Phys.*, **68** (2005) 577.

[33] KRASNOV V. M., *Phys. Rev. B*, **83** (2011) 174517.

[34] VIRKAR Y. and CLAUSET A., *Ann. Appl. Stat.*, **8** (2014) 89.

[35] KRETSCHMER M., KHRAPAK S. A., ZHDANOV S. K., THOMAS H. M., MORFILL G. E., FORTOV V. E., LIPAEV A. M., MOLOTKOV V. I., IVANOV A. and TURIN M., *Phys. Rev. E*, **71** (2005).

[36] SCHWABE M., RUBIN-ZUZIC M., ZHDANOV S., THOMAS H. M. and MORFILL G. E., *Phys. Rev. Lett.*, **99** (2007) 095002.

[37] RUMPF B., NEWELL A. C. and ZAKHAROV V. E., *Phys. Rev. Lett.*, **103** (2009) 074502.

[38] MANN J. A. jr. and HAUSEN R. S., *J. Colloid Sci.*, **18** (1963) 757.

[39] WHITHAM G. B., *Linear and Nonlinear Waves* (J. Wiley, New York) 1974.

[40] FRISCH U., *Turbulence: The Legacy of A.N. Kolmogorov* (Cambridge University Press) 1995.

[41] BENZI R., CILIBERTO S., TRIPICCIONE R., BAUDET C., MASSAIOLI F. and SUCCI S., *Phys. Rev. E*, **48** (1993) R29.

[42] KOLMOGOROV A. N., *C. R. Acad. Sci. URSS*, **30** (1941) 301.

[43] NUNOMURA S., ZHDANOV S., MORFILL G. E. and GOREE J., *Phys. Rev. E*, **68** (2003) 026407.

[44] BURTON L. M., COHEN J. A., PRADIPTA R., LABNO A., LEE M. C., BATISHCHEV O., ROKUSEK D. L., KUO S. P., WATKINS B. J. and OYAMA S., *Phys. Scr.*, **T132** (2008) 014030.

[45] RUMPF B. and NEWELL A. C., *Phys. Lett. A*, **377** (2013) 1260.

[46] LIGHTHILL M. J., *Proc. R. Soc. A*, **299** (1967) 28.

[47] BOFFETTA G. and MUSACCHIO S., *Phys. Rev. E*, **82** (2005) 016307.

[48] KRAICHNAN R. H., *Phys. Fluids*, **10** (1967) 1417.

[49] CHERTKOV M., CONNAUGHTON C., KOLOKOLOV I. and LEBEDEV V., *Phys. Rev. Lett.*, **99** (2007) 084501.

[50] VLADIMIROVA N., DEREVYANKO S. and FALKOVICH G., *Phys. Rev. E*, **85** (2012) 010101(R).

[51] CONNAUGHTON C., NAZARENKO S. and NEWELL A. C., *Physica D*, **184** (2003) 86.